Aerobiologia (2015) 31:421–434
DOI 10.1007/s10453-015-9375-5

ORIGINALPAPER

Airborne-pollen maps for olive-growing areas throughout the Mediterranean region: spatio-temporal interpretation

Fátima Aguilera · Ali Ben Dhiab · Monji Msallem · Fabio Orlandi · Tommaso Bonofiglio · Luis Ruiz-Valenzuela · Carmen Galán · Consuelo Díaz-de la Guardia · Angelo Giannelli · María del Mar Trigo · Herminia García-Mozo · Rosa Pérez-Badia · Marco Fornaciari

Received: 12 September 2014 / Accepted: 17 March 2015 / Published online: 22 March 2015

Abstract The aim of this study was the elaboration and the spatio-temporal interpretation of *Olea europaea* L. airborne-pollen maps across the main olive cultivation areas within the Mediterranean basin (i.e. Tunisia, Spain, Italy). The study was performed using aerobiological databases recorded from 27 georeferenced study sites. Maps were elaborated for different 10-day period through spring and summer: 1, 10, 20, 30 April; 10, 20, 30 May; 9, 19, 30 June; and 10 July. Average pollen counts in each study site were considered for the 13-year period from 1999 to 2011. Both these 10-day period of pollen emission data and the geographical coordinates were used as variables in the elaboration of the 10-day period maps. The 'Natural Neighbour' interpolation method was used. The statistical relationship between spatial location and maximum pollen emission was studied using linear regression and cluster analyses. The airborne-pollen maps show a spatio-temporal pattern in the pollen season. The maximum pollen emission is progressively delayed with northward changes in latitude, and the classification of the *Olea* maximum pollen emission date into four latitudinal categories is defined. The maximum *Olea* pollen concentrations

F. Aguilera (✉) · F. Orlandi · T. Bonofiglio · A. Giannelli · M. Fornaciari
Department of Civil and Environmental Engineering, University of Perugia, Borgo XX Giugno 74, 06121 Perugia, Italy
e-mail: faguiler@ujaen.es

A. B. Dhiab · M. Msallem
Institut de l'Olivier, BP 208, 1082 Tunis, Tunisia

L. Ruiz-Valenzuela
Department of Animal Biology, Plant Biology and Ecology, Agrifood Campus of International Excellence (CeiA3), University of Jaen, Campus of the Lagunillas s/n, 23071 Jaén, Spain

C. Galán · H. García-Mozo
Department of Botany, Ecology and Plant Physiology, Agrifood Campus of International Excellence (CeiA3), University of Cordoba, Campus of Rabanales, 14071 Córdoba, Spain

C. Díaz-de la Guardia
Department of Botany, University of Granada, Avda. Fuentenueva, 18071 Granada, Spain

M. del Mar Trigo
Department of Plant Biology, University of Malaga, Campus of Teatinos, 29071 Málaga, Spain

R. Pérez-Badia
Institute of Environmental Sciences, University of Castila La-Mancha, Avda. Carlos III, Toledo, Spain

were mainly recorded around 20 May. Early flowering in Tunisia coastal zones can indicate the onset of the olive pollen release season in the occidental Mediterranean region, while the central olive-growing areas in Italy can indicate the end of the olive pollen release season. These maps give information of the major risk days to the people who are allergic to olive pollen.

Keywords Airborne-pollen maps · Geostatistics · Latitude · Mediterranean region · Olive · Pollinosis

1 Introduction

Olive groves constitute a fundamental part of the Mediterranean environment and its culture and economy, as the olive fruit and oil are among the oldest and most important products in this area (Barranco et al. 2008). Over 750 million olive trees are cultivated worldwide, 95 % of which are in the Mediterranean region (International Olive Council 2012). Spain is the largest olive oil-producing country, followed by Italy, Greece and Tunisia. Together, these four countries produce 80 % of the total world olive oil production. According to the Food and Agriculture Organisation (2013), the world olive cultivation area tripled between 1960 and 1998, from 2,600,000 hectares to 7,950,000 hectares, and reached 10,244,194 hectares in 2013.

Olive pollen has become the most abundant type of pollen within the pollen spectrum, due both the notable increase in its cultivation area and to the intense flowering of the trees, which release abundant amounts of pollen grains into the atmosphere during spring (García-Mozo et al. 2008; Aguilera and Ruiz-Valenzuela 2012). The pollen emitted by olive trees is considered as one of the main causes of respiratory allergic disease in the Mediterranean basin (D'Amato et al. 2007). In countries of olive cultivation vocation as Spain, Italy, Greece or Turkey, olive pollen is the most important cause of pollinosis, provoking seasonal allergic rhinitis and bronchial asthma among the population (D'Amato et al. 2007).

Aerobiological information has been successfully used to analyse the olive flowering phases, with airborne-pollen data used as a well-proven tool for indirect evaluation of the flowering period (Galán et al. 2008; Aguilera and Ruiz-Valenzuela 2009). Furthermore, the close relationship between pollen emission and fruit production has been shown to be a good tool for crop forecasting models of numerous anemophilous plant species, and optimal yield forecasting models have been defined for olive groves in several Mediterranean countries (Galán et al. 2008; Orlandi et al. 2010; Oteros et al. 2013).

The Mediterranean region has been identified as one of the most prominent world 'hot-spots', with warming trends and spatial variability of the rainfall regimes expected in the future (Giorgi and Lionello 2008). Changes in the climate would potentially result in a serious imbalance of the biological rhythms of plant species. It is assumed that cultivation of the olive tree defines the climate. However, the effects of climate change on Mediterranean olive-growing areas might depend on how these changes in temperature and rainfall pattern occur. The physiological processes throughout the life cycle of the olive plant are affected by the climate (Bonofiglio et al. 2009; Aguilera et al. 2014). In particular, the reproductive phenology of the olive tree, and especially the flowering period, can be considered as a sensitive bio-indicator of the impact of future climate change (Moriondo et al. 2013; Orlandi et al. 2014).

Geostatistics is a branch of statistics that focuses on spatial and spatio-temporal datasets. Few studies have considered the inclusion of biological variables together with the 'space' variable, probably due to a lack of long spatio-temporal data series. According to León-Ruiz et al. (2012), georeferenced data can be incorporated into a geographical information system (GIS) to produce map layers. In addition, geostatistics is strongly related to interpolation methods. Over the last few years, different interpolation techniques have been developed to estimate data for a whole region from data collected at only a few sites, and consequently, bio-spatial analysis is being successfully developed on local and regional scales (Alba et al. 2006; León-Ruiz et al. 2012).

The aim of the present study was the elaboration and interpretation of olive airborne-pollen maps within the Mediterranean region. The construction of pollen emission maps can be considered as a fundamental complement for the interpretation of *Olea* airborne-pollen dynamics, which is not only useful because of their allergenic potential, but also essential for any evaluation of the effects of climatic change on the behaviour and management of agro-ecosystems such as the olive grove.

2 Materials and methods

2.1 Study area

The study was performed in the Mediterranean region, in terms of three of the main olive oil production countries on the world: Spain, Italy and Tunisia. The main olive-growing areas were considered in these countries (Fig. 1). In this region, the rainfall pattern is characterised by seasonality and by annual variability (Giorgi and Lionello 2008). The annual mean temperatures are between 17.0 °C (Italy study area) and 20.3 °C (Tunisia study area). The annual rainfall ranges from 288 mm (Tunisia study area) to 657 mm (Italy study area) (Table 1).

2.2 Aerobiological survey

This study was performed using aerobiological databases. The olive pollen sampling activities were carried out using the volumetric method, which is based on capturing the pollen and other biological particles present in the air (European Aerobiology Society Quality Control Working Group 2011). The monitoring traps were inside or near to olive groves, for the detection of the pollen from a wide olive-growing area (Orlandi et al. 2010). Pollen emission data were collected over a 13-year period (1999–2011).

The main pollen season was determined using a modification of the criteria described by Galán et al. (2001). The start of the pollen season was defined as the first day on which at least five pollen grains m^{-3} were collected, with the subsequent days at $\geq$5 pollen grains m^{-3}. The end of the season was the last day on which five pollen grains m^{-3} were collected, when the subsequent days had concentrations <5 pollen grains m^{-3}. The most relevant data that were recorded during the main olive pollen season, as the means for each of the three countries, were as follows: start and end dates of the pollen season; duration (in days) of the pollen season; and date of maximum daily pollen concentration (i.e. peak pollen emission date).

2.3 Pollen emission maps

The evolution of the olive pollen season with time and space throughout the Mediterranean region was analysed through the elaboration of the airborne-pollen maps, which were elaborated for different 10-day period through spring and summer: 1, 10, 20, 30 April;

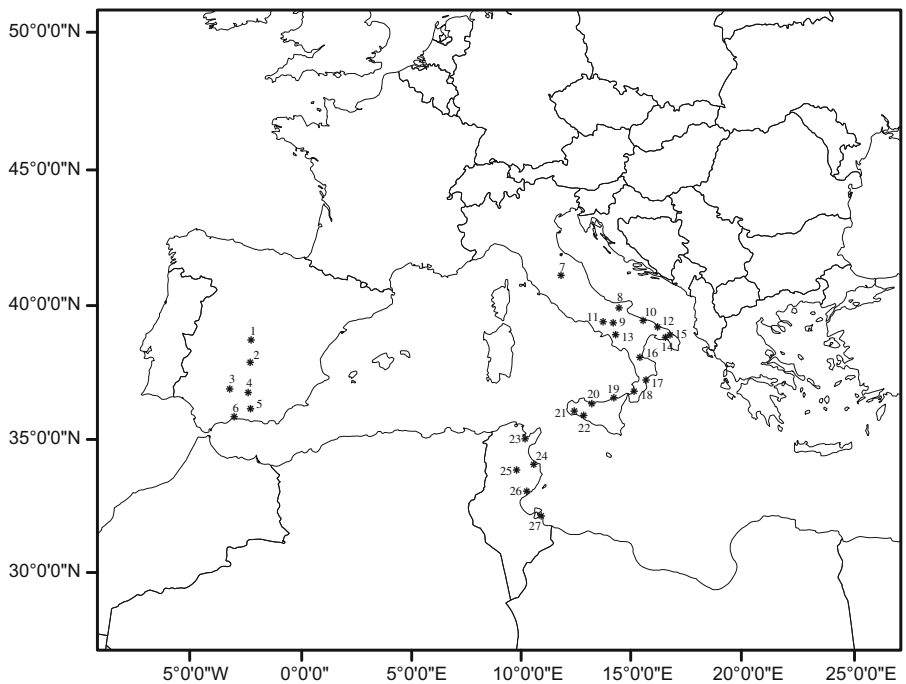

Fig. 1 Locations of the study sites. Numbers correspond to study sites given in Table 1

Table 1 Main features of each study site

Study site	Map ref.[a]	Coordinates	Altitude (m a.s.l.)	Tmean (°C)	Rainfall (mm)	Sampling period
Spain						
Toledo	1	39°51′N, 04°02′W	529	15.9	348	2003–2011
Ciudad Real	2	38°59′N, 03°55′W	623	15.8	422	1999–2011
Cordoba	3	37°50′N, 04°45′W	123	18.3	590	1999–2011
Jaen	4	37°48′N, 03°48′W	568	17.1	485	1999–2011
Granada	5	37°11′N, 03°35′W	685	15.9	394	1999–2011
Malaga	6	36°47′N, 04°19′W	5	18.7	537	1999–2011
Italy						
Perugia	7	43°06′N, 12°23′E	450	14.2	829	1999–2011
Foggia	8	41°25′N, 15°33′E	57	16.1	363	1999–2011
Benevento	9	41°07′N, 14°50′E	152	16.3	846	1999–2011
Bari	10	41°03′N, 16°38′E	191	16.2	571	1999–2011
Avellino	11	40°55′N, 14°47′E	29	14.6	788	1999–2011
Brindisi	12	40°52′N, 17°01′E	230	17.4	703	1999–2011
Salerno	13	40°37′N, 14°52′E	29	15.1	888	1999–2011
Taranto	14	40°28′N, 17°13′E	104	15.2	891	1999–2011
Lecce	15	39°49′N, 18°21′E	48	16.3	441	1999–2011
Cosenza	16	39°43′N, 16°10′E	10	17.8	443	1999–2011
Catanzaro	17	38°58′N, 16°16′E	216	18.9	922	1999–2011
Reg. Calabria	18	38°14′N, 15°39′E	11	19.4	440	1999–2011
Messina	19	38°12′N, 14°75′E	59	19.4	786	1999–2011
Palermo	20	38°11′N, 13°06′E	21	18.9	367	1999–2011
Trapani	21	37°40′N, 12°46′E	7	19.4	786	1999–2011
Agrigento	22	37°30′N, 13°31′E	158	17.1	453	1999–2011
Tunisia						
Mornag	23	36°39′N, 10°16′E	40	19.4	463	1999–2011
Jemmel	24	35°38′N, 10°41′E	30	20.1	305	1999–2011
Menzel	25	35°25′N, 09°50′E	160	21.0	279	1999–2011
Chaal	26	34°34′N, 10°19′E	97	20.0	223	1999–2011
Zarzis	27	33°35′N, 11°01′E	17	21.2	170	1999–2011

[a] See Fig. 1

Tmean mean annual temperature

10, 20, 30 May; 9, 19, 30 June; and 10 July (1, 9, 10, first 10-day period of the month; 19, 20, second 10-day period of the month; 30, third 10-day period of the month). The pollen concentrations (as pollen grains m^{-3} air) for this 10-day period were calculated as the average pollen counts across the 5 days before and the 5 days after the given date. The average pollen counts for the period 1999–2011 were used for each study site. Both the 10-day period pollen emission data and the geographical coordinates were used as variables in the elaboration of the 10-day period maps.

As only a few monitoring sites were available, interpolation values for unsampled points were obtained. In the present study, the natural neighbor interpolation method was used. Different averaging functions yield a variety of natural neighbor interpolations. Among them, Sibson's method is the most commonly used (Sibson 1981). This method uses the observed data from sampling sites and estimates values for coordinates where no such station exits but which can be correlated with a specific spatial domain. To check the reliability of the interpolation

described here, cross-validation analyses were performed. The numerical information produced is then inserted inside the digital cartography system, with the plotting of the final airborne-pollen maps. These maps were firstly elaborated for each country, and later integrated across all of the countries, to provide a single Mediterranean map. The maximum pollen concentrations for each country are indicated on the maps in dark blue, with the darkest colour corresponding to the maximum values (see Fig. 2, legend).

Linear regression analysis and correlation analysis (parametric or nonparametric according to data normality) were performed to establish the statistical relationships between geographical/meteorological variables (i.e. the latitude, the altitude, the mean annual temperature and the total annual precipitation) and the maximum pollen emission (peak pollen emission date), using the available average data for each study site. In the same way, cluster analysis was performed to establish the statistical relationships between the spatial locations (latitude) and the maximum pollen emission (peak pollen emission date). The ArcGIS 10.0 and STATISTICA 7.0 (StatSoft Inc., USA) software packages were used.

2.4 Long-term trends analysis

Analysis of long-term trends in both the peak pollen emission date (day of the year; DOY) and the maximum daily pollen concentration (pollen grains m^{-3} air) for each study site during the entire period 1999–2011 was performed using Mann–Kendall tests, which are non-parametric tests for detecting the presence of monotonic increasing or decreasing trends. The trends were evaluated using the Z coefficient estimation for every variable considered. A positive or negative *Z*-value indicates the presence of an increasing or decreasing trend within a data series, respectively. To estimate the true slope of any existing trend, the Sen's nonparametric method was used (Sirois 1998). The Excel template application MAKESENS version 1.0 (Salmi et al. 2002) was used for the Mann–Kendall trend analysis.

3 Results

3.1 Mean olive pollen release season

The pollen release season of the olive tree across the study area spanned mainly from the middle of April to the end of June (Table 2), with different temporal patterns detected. During the study period, 12 April was the average start date in the Tunisian study area, followed by Spain on 23 April and Italy on 3 May. Similarly, temporal fluctuations were evident for the peak pollen emission dates. In the Tunisian study area, the average maximum pollen emission date was 27 April, while for the Spanish and Italian study areas, this was 19 May and 23 May, respectively. The duration of the main pollen release season also showed variations between the three areas. The longest main pollen release season was in Spain, with an average of 67 days. The main pollen release season was shortest in Tunisia, at 42 days, and was 51 days in Italy.

3.2 Olive airborne-pollen maps

The first pollen grains were detected on 1 April in the central northern coastal zones of Tunisia (Fig. 2a). Ten days afterwards, the pollen release season had extended towards the internal zones of Tunisia, where the average maximum pollen concentrations reached 90 grains m^{-3} air, while the first pollen grains in the south coastal areas of Spain were recorded (Fig. 2b). For the second 10-day period of April (20 April), the pollen levels increased considerably in central Tunisia, where the pollen release season became more intense. In south-western Spain for this 10-day period, the pollen reached a maximum of 100 grains m^{-3} air. Simultaneously, the first pollen grains were recorded for southern Italy (Sicily) (Fig. 2c). The highest pollen levels in the Tunisian study area were recorded for the third 10-day period of April (30 April) (Fig. 2d). The Jemmel, Menzel and Chaal study sites, that are located in the central and northern Tunisian olive-growing areas, provided the maximum airborne-pollen levels, which reached >555 grains m^{-3} air (Fig. 3a). A notable increase in the average pollen levels recorded in the south-west areas of Spain and Italy also occurred at this time.

The pollen emission map constructed with the data for the first 10-day period of May (10 May) shows high pollen concentrations all three of the countries, but above all in the southern olive-growing areas of Spain and Italy (Fig. 2e). For Spain, in this period, the maximum pollen concentrations were between 700 and 1770 grains m^{-3} air, which were recorded for the Cordoba and Jaen study sites. In Italy, Trapani study site reached a maximum absolute value of 635 grains

m^{-3}. In northern Tunisia, the pollen levels ranged from 200 to 450 grains m^{-3} air during this period (Fig. 2e).

The highest pollen levels in both Spain and Italy were reached for the second 10-day period of May (20 May), which showed maximum averages of 932 and

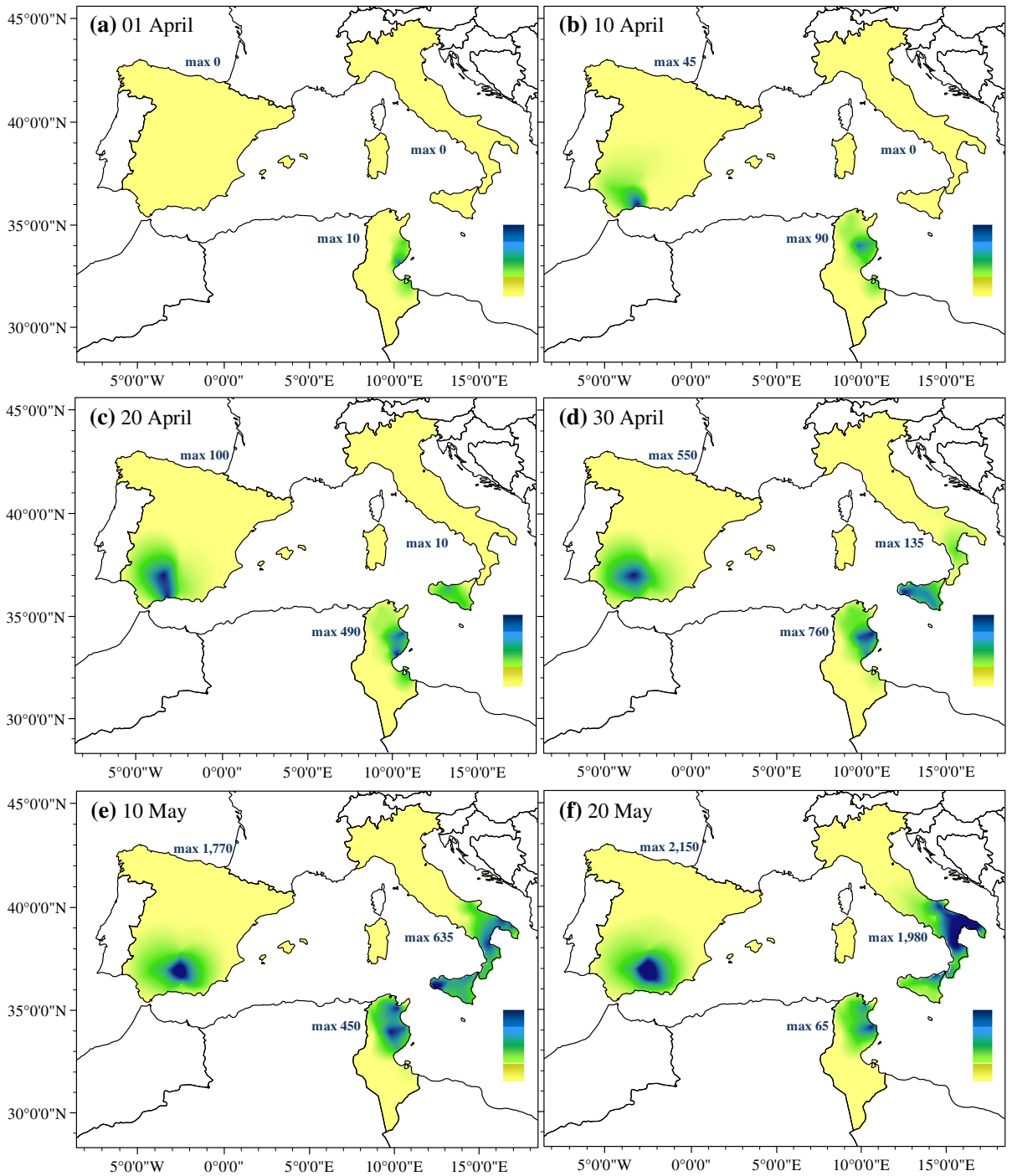

Fig. 2 Ten-day period airborne-pollen maps through the olive pollen release season for the study countries. The maximum (max) 10-day period of pollen emission is shown for each country

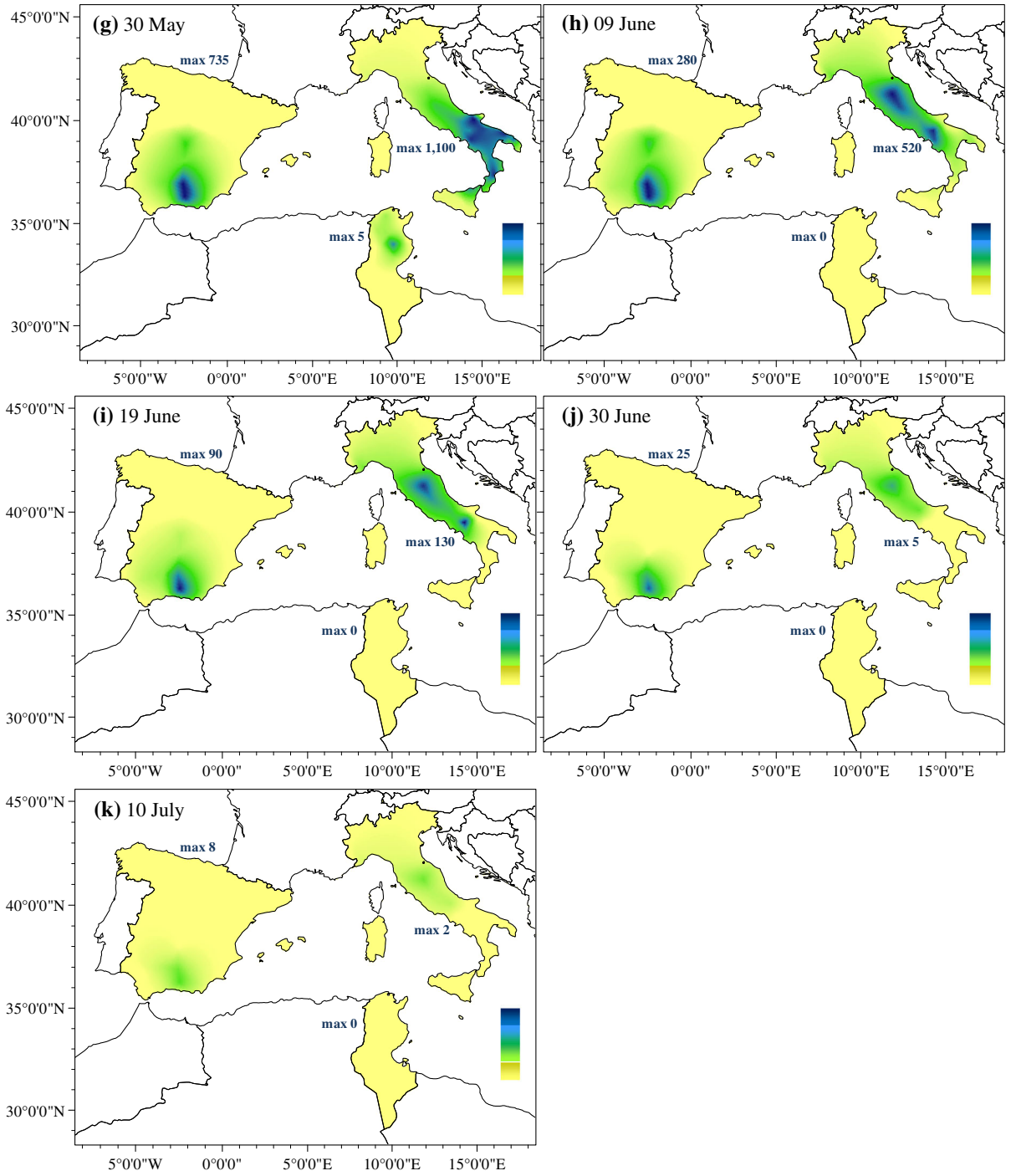

Fig. 2 continued

835 grains m^{-3} air, respectively (Fig. 2f). The highest pollen concentrations were seen for the south-eastern olive-growing areas of Spain (Jaen study site: maximum absolute value, 2147 grains m^{-3} air) and south-eastern areas of Italy (Brindisi study site: maximum absolute value, 1980 grains m^{-3} air) (Fig. 3b, c). During this period, the airborne-pollen concentrations decrease notably in the Tunisian study sites.

Table 2 Main characteristics of the pollen season of *Olea europaea* L. for each country in the study area

Country	Pollen release season				
	Start date	End date	Duration (days)	Peak date	10-day period "peak date"
Tunisia	12 April	23 May	42 ± 6	27 April	30 April
Spain	23 April	28 June	67 ± 9	19 May	20 May
Italy	3 May	22 June	51 ± 5	23 May	20 May

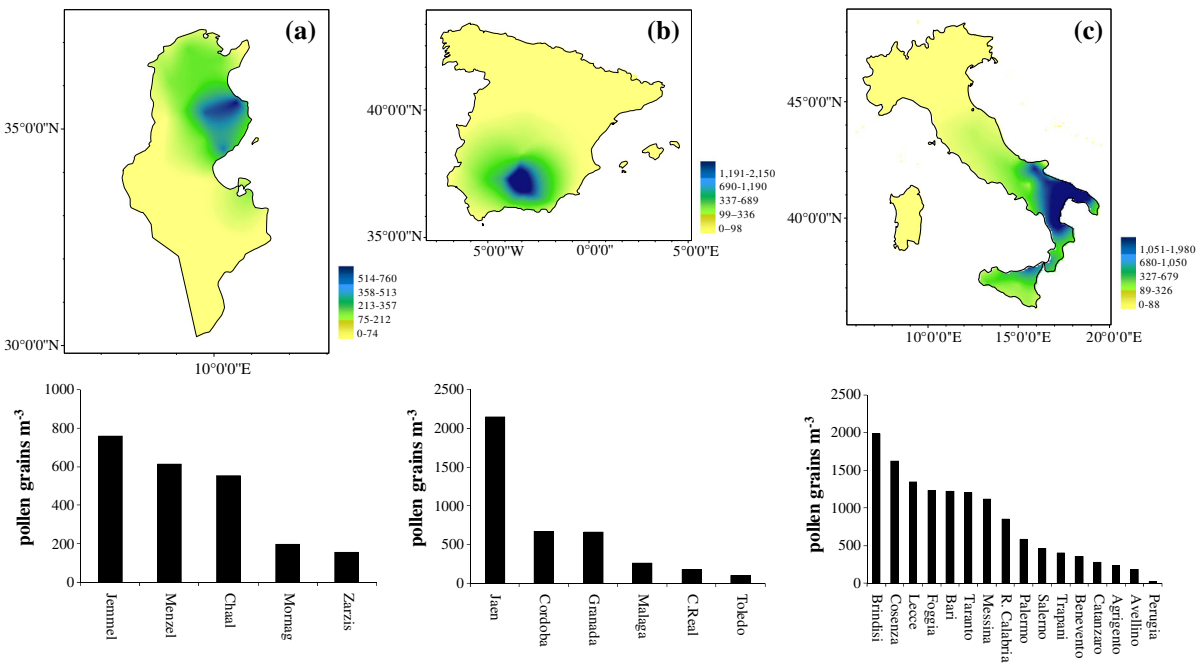

Fig. 3 Ten-day period airborne-pollen maps for maximum olive pollen emission, and histograms of individual maximum olive pollen emission according to the individual georeferenced study sites in Tunisia (**a**, 30 April), Spain (**b**, 20 May) and Italy (**c**, 20 May)

For the successive days, progression of the pollen release season towards the central areas of Spain and Italy was clearly seen (Fig. 2g). In early June, the pollen release season was more intense in both the interior zones of central Italy and the higher latitudinal/altitudinal areas of central south-eastern Spain, while in Tunisia, the pollen release season of the olive was completely finished (Fig. 2h). A few days later, and on towards the end of June, the pollen release season was practically finished in the other areas, with airborne-pollen concentrations below 25 grains m^{-3} air (Fig. 2i, j).

Results of the cross-validation analysis are shown in Table 3. The regression coefficient represents a measure of the goodness of fit for the model describing the linear regression equation. In general, the regression coefficients were close to 1, mainly for the 10-day period dates with higher pollen emission concentrations, such as can be seen in the Fig. 4 that shows the goodness of the fit of the estimated values for the periods of maximum pollen emission in each country. These cross-validation results corroborate the efficiency of the estimation method used for the interpolation.

Figure 5 (dotted line) shows the cumulative pollen emissions recorded contemporarily across the entire Mediterranean study area. Figure 5 also includes the polynomial trend line constructed with the cumulative pollen emissions, as represented by a parabolic curve similar to a Gaussian 'bell' curve (Fig. 5, solid line). According to the results, the olive pollen emission in the study area is statistically 'normally distributed',

Table 3 Cross-validation summary results

	Regression coefficient		
	Tunisia	Spain	Italy
1 April	0.44	–	–
10 April	0.60	0.68	–
20 April	0.57	0.67	0.67
30 April	0.93	0.89	0.55
10 May	0.91	0.88	0.73
20 May	0.81	0.94	0.72
30 May	0.13	0.89	0.76
09 June	–	0.91	0.82
19 June	–	0.72	0.66
30 June	–	0.53	0.21
10 July	–	0.51	0.16

being relatively symmetrically distributed about their mean (which occurred on 20 May).

3.3 Relationships between maximum pollen emission and spatial locations

The simple linear regression results are shown in Fig. 6. A significant and strongly positive relationship was found between the peak pollen emission date and the latitude, with an R^2 of 0.75 ($p < 0.05$) (Fig. 6a). This relationship was weak and not significant regarding the altitude, with an R^2 of 0.14 (Fig. 6b). A significant and negative relationship was also found between the peak pollen emission date and the mean annual temperature (Fig. 6c), with an R^2 of 0.65 ($p < 0.05$), being this relationship positive regarding the total annual precipitation, with an R^2 of 0.44 ($p < 0.05$) (Fig. 6d).

The correlation analysis showed as the variable "latitude" is significantly and positively related to both the peak pollen emission date ($r = 0.86, p < 0.05$) and the total annual precipitation ($r = 0.63, p < 0.05$). This relationship was significantly negative regarding the mean annual temperature ($r = -0.83, p < 0.05$).

Cluster analysis classifies the study sites into four latitudinal categories (Fig. 7). The first latitudinal category includes the Tunisian study sites (Fig. 7, A), which have a mean latitude of 35°34′N and a mean peak pollen emission date of 27 April (DOY 117). The second latitudinal category mainly includes the warmer Spanish sites and the Sicilian territories (Fig. 7, B), which have a mean latitude of 37°38′N and a mean peak pollen emission date of 12 May (DOY 132). Fourteen study sites are included in the third latitudinal category (Fig. 7, C), and these correspond to the central Spanish and Italian areas, with a mean latitude of 39°31′N and a mean peak pollen emission date of 24 May (DOY 144). Finally, the fourth latitudinal category (Fig. 7, D) includes just two Italian study sites, with a mean latitude of 41°31′N and a mean peak pollen emission date of 6 June (DOY 157).

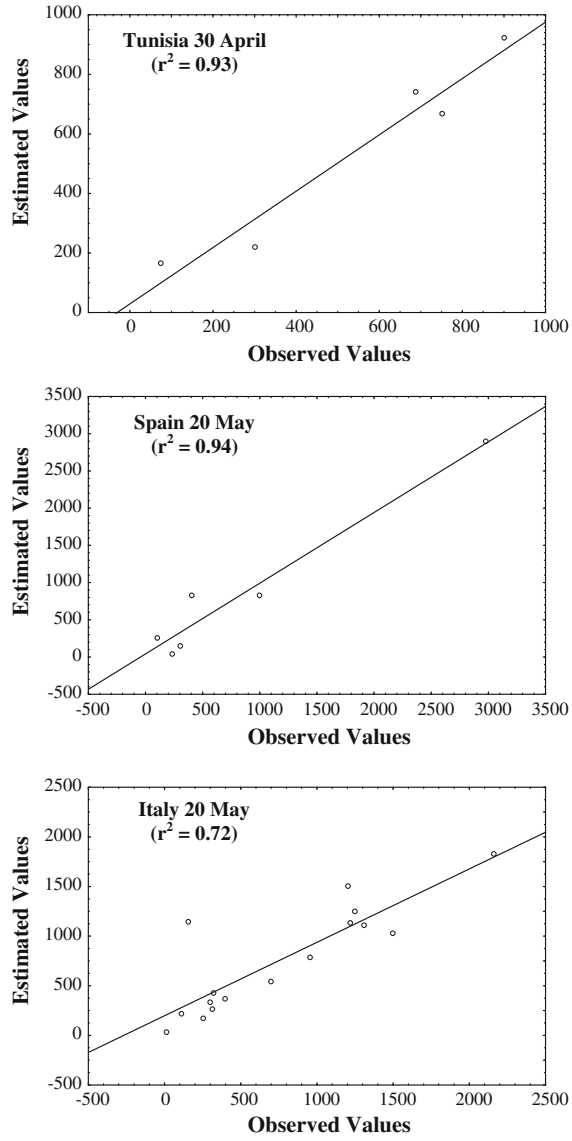

Fig. 4 Cross-validation analyses obtained for the 10-day period of maximum pollen emission in each country

3.4 Long-term trends analysis results

The main features of the Mann–Kendall tests for the entire period 1999–2011 are summarised in Table 4. The peak pollen emission date showed a decreasing tendency in all the Spanish and Tunisian areas, although significant *Z*-values were not found, only in Ciudad Real study site, where a significant advance of 1 day per year was recorded. However, the tendency is not so clear in Italy, where decreasing and increasing trends were detected and only two significant increasing trends were observed in Taranto and Calabria study sites. The peak pollen concentrations recorded for the Italian, and the Tunisian sites showed a general decreasing but non-significant tendency. On the contrary, notable increasing trends in the peak pollen concentrations of three of the Spanish study sites were confirmed with the large and significant positive *Z*-values obtained. According to the results, the maximum pollen concentrations showed a significant increase ranging between 46 and 292 grains of pollen m^{-3} of air per year.

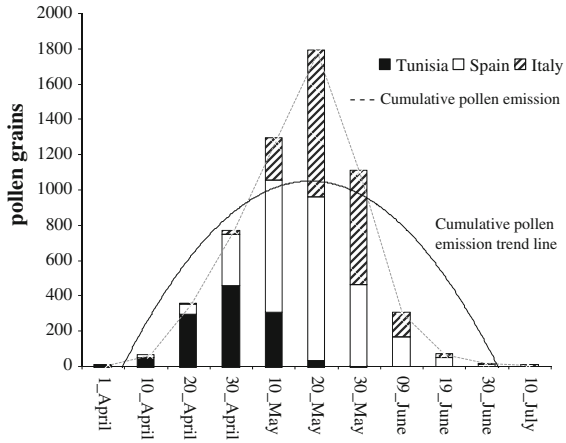

Fig. 5 Cumulative olive pollen emissions for Tunisia, Spain and Italy through the olive pollen release season (histogram, *dotted line*). The cumulative pollen emission trend line is also shown (*solid line*)

4 Discussion

The maps presented in this study provide a picture of the olive pollen spatial distributions in several areas of the Mediterranean region. The use of both the

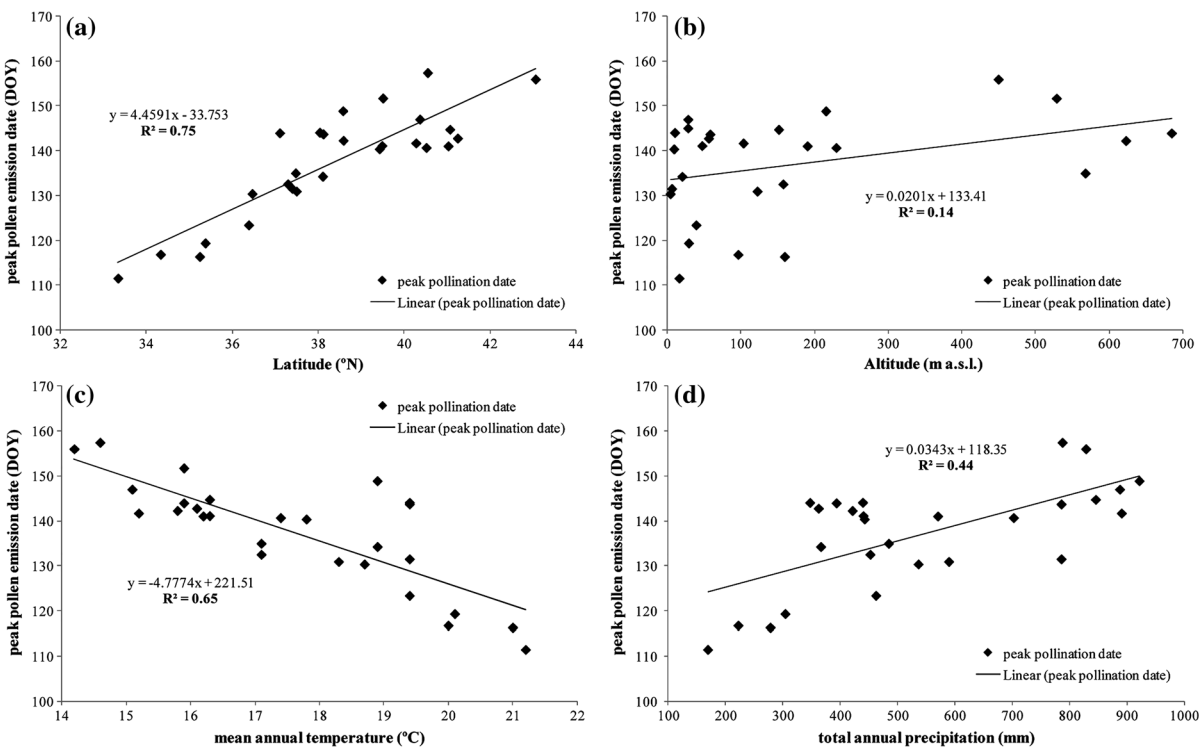

Fig. 6 Linear fit (*solid line*) of the regression analysis between the latitude (**a**), altitude (**b**), mean annual temperature (**c**), total annual precipitation (**d**) and peak olive pollen emission data (*filled diamonds*), according to the day of the year (DOY)

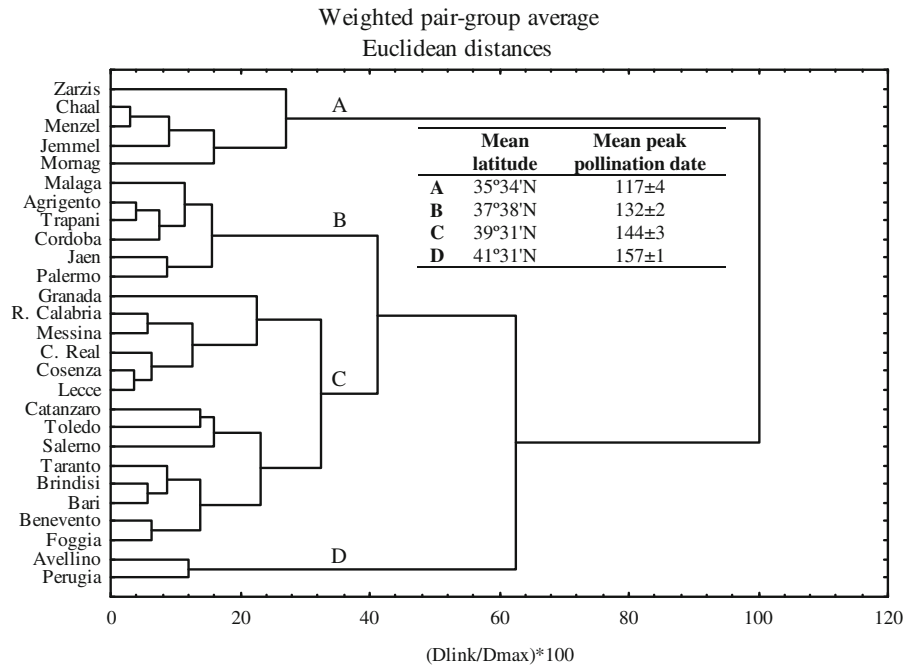

Fig. 7 Dendrogram generated according to cluster analysis, indicating the four spatio-temporal latitudinal categories according to the mean peak pollen emission dates (*A–D*)

georeferenced data and the interpolation method has allowed the estimation of the airborne-pollen concentrations for a whole region from data collected from a few monitoring sites. Real and estimated values can consequently be used to map the airborne-pollen variations through a spatio-temporal scale.

These airborne-pollen maps present a two-dimensional view of the study region and show a step-wise pollen release season. The first olive pollen grains were detected in the warmest Mediterranean areas, with the progression of the pollen release season towards the internal Mediterranean areas, which have a continental climate. The relationships between the location and behaviour of the pollen release season in plant species such as olive or grasses have been widely studied (Galán et al. 2008; Bonofiglio et al. 2009; León-Ruiz et al. 2012; Oteros et al. 2013). The step-wise pollen release season detected in this study is in agreement with previous regional studies for the olive tree (Orlandi et al. 2005; Alba et al. 2006). The latitude-induced microclimatic conditions determine the physiological responses of olive trees. In particular, the peak pollen emission date, which corresponds to the day on which most of the tree canopy flowers are open, is influenced strongly by this factor. This relationship has already been detected in a previous and recent study carried out throughout the Mediterranean area (Aguilera et al. 2014). The olive groves located in the northern areas need more time than those in more central/southern areas to completely satisfy their biothermic requirements, with these being notably higher than those in the warmest areas. Thus, the olive trees in the Tunisian areas are the first to complete flower development and to begin their flowering season, and consequently, they are the first to emit their pollen into the atmosphere.

The findings herein confirm that the latitude is strongly related to the maximum olive pollen emission date and the mean annual temperature. Moreover, this relationship is significant, although weaker, regarding to the total annual precipitation. The regimes of temperature and the precipitation, meteorological variables closely related to the biological reproductive cycle of the olive tree (Galán et al. 2008; Aguilera and Ruiz-Valenzuela 2012; Orlandi et al. 2014), are indirectly reflected in the "latitude" values. For this reason, this geographical variable could be successfully used as bio-spatial classifier. In the present study, the classification of the maximum olive pollen emission date into four latitudinal categories was established. The first latitudinal category corresponds to the warmest of the study areas, i.e. the Tunisian olive-growing areas, where the peak pollen emission occurred in late April. Moving to the middle of May,

Table 4 Summary of the main features of the Mann–Kendall trends (1999–2011)

Study site	Peak date (DOY)			Peak pollen (pollen grains m^{-3})		
	Test *Z*	Sign.	Sen's slope estimate (Q)	Test *Z*	Sign.	Sen's slope estimate (Q)
Toledo	−0.40		−0.09	0.87		97.95
Ciudad Real	−2.26	*	−1.25	2.02	*	45.80
Cordoba	−0.73		−0.75	3.48	***	291.81
Jaen	−0.31		−0.17	−0.75		−97.20
Granada	−0.37		−0.20	2.38	*	134.95
Malaga	−0.43		−0.57	−0.43		−25.62
Perugia	−0.37		−0.31	−0.67		−4.57
Foggia	0.43		0.17	−0.18		−71.81
Benevento	1.04		0.29	0.03		4.58
Bari	−0.97		−0.40	1.10		170.70
Avellino	−0.06		−0.06	−0.62		−68.32
Brindisi	0.80		0.35	−0.62		−131.57
Salerno	−0.06		−0.07	−0.16		−41.17
Taranto	2.59	**	0.65	−0.62		−192.19
Lecce	−1.05		−0.50	−0.43		−141.85
Cosenza	−0.68		−0.32	−0.55		−178.47
Catanzaro	0.12		0.21	0.31		65.67
Reg. Calabria	1.85	+	0.78	−0.06		−5.88
Messina	1.22		0.82	−0.07		−23.99
Palermo	1.45		1.00	1.30		149.70
Trapani	−0.67		−0.33	0.48		59.37
Agrigento	−1.60		−0.71	−0.55		−23.16
Mornag	−0.99		−0.24	−0.44		−85.08
Jemmel	−0.31		−0.28	−0.47		−102.00
Menzel	−0.25		−0.10	−0.06		−17.02
Chaal	−0.67		−0.35	−0.62		−105.00
Zarzis	−0.74		−0.42	−0.67		−83.65
Spain	−0.73		−0.38	0.86		34.18
Italy	0.31		0.04	−0.07		−6.61
Tunisia	−0.74		−0.27	−1.03		−107.08

DOY day of the year

$^{+}$ $p \leq 0.1$; * $p \leq 0.05$; ** $p \leq 0.01$; *** $p \leq 0.001$; blank cell, not significant *Z* value

the maximum pollen emission was recorded for the warmer areas of southern Spain and the island of Sicily. Some days afterwards, towards the end of May, the maximum pollen emission was recorded for the central Mediterranean study areas that are included into the third latitudinal category, i.e. central Spain and southern central Italy. A notably delay in the pollen release season of the olive groves located at higher latitudes or in colder areas was detected. These areas, which are included into the fourth latitudinal category, showed their maximum pollen emission in the first week of June. Therefore, the early flowering in the Tunisian coastal zones might serve as an indicator of the onset of the olive pollen release season in the occidental Mediterranean region, while the central olive-growing areas in Italy can be used to establish the end of the olive pollen release season. Given that the content of the olive pollen in the atmosphere shows different spatio-temporal patterns, the maps presented in this study are especially relevant for people who are

allergic to olive pollen, which is the main cause of seasonal allergy in the Mediterranean basin (D'Amato et al. 2007).

From a quantitative point of view, spatial fluctuations in the pollen concentrations were also detected. In general, southern Spain showed the highest olive pollen emission, followed by southern Italy and central northern Tunisia. The maximum pollen concentrations in southern Spain occurred when the olive groves of Cordoba, Granada, and especially Jaen, were in full flowering. These olive-growing areas occupy a large land surface, and they are considered as the most extensive olive oil-producing areas in Spain (Barranco et al. 2008).

For Italy, the maps show that the olive groves of the Puglia, Calabria and Campania Regions, together with the olive-growing areas of northern Sicily, contribute the most to the higher pollen concentrations in the air. These regions represent more than 90 % of the productive Italian olive groves (Bonofiglio et al. 2009). The lowest pollen emission was recorded for Tunisia, mainly due to the olive tree cultivation, which covers one-third of the arable land, and is thus less widespread in these semi-arid areas.

Although a time period long enough has not been considered, interesting trends in both the peak pollen emission dates and the maximum daily pollen concentrations were observed. Decreasing trends in the peak pollen emission dates of the olive trees located in Spain, Tunisia and numerous Italian areas were detected. These data are in agreement with previous studies that have detected earlier mean flowering dates in numerous plant species within European countries (Bonofiglio et al. 2009; García-Mozo et al. 2014; Menzel and Sparks 2006). The trend is not so clear regarding the pollen emission process. The olive pollen emissions are decreasing in the Tunisian and some of the Italian areas. On the contrary, significant increasing trends were detected in south Spain, such as has been recently reported by García-Mozo et al. (2014). The warming tendency observed in the Mediterranean region is strongly related to the anticipation of the full flowering period in the olive tree, and it therefore appears reasonable that this phenological stage might manifest particular sensitivity to future global climate change (Giorgi and Lionello 2008; Orlandi et al. 2014). Inconsistent results regarding the airborne-pollen trends do not allow any firm conclusions here, and therefore, further studies are needed.

Under the context of climate change, airborne-pollen maps can be used to visualise spatio-temporal changes in the progression of the olive pollen release season through the Mediterranean region. Notable tendencies towards increased temperatures and evapotranspiration, together with lower rainfall patterns, have been detected in this region, and as a consequence, the fundamental vegetative and reproductive phases of numerous plant species, included the olive tree, might have serious problems in their adaptation to new climate scenarios (Giorgi and Lionello 2008; Moriondo et al. 2013; Orlandi et al. 2014). In this sense, it would be interesting to plot maps with climatic projections in the coming decades under different emission scenarios, to model the biological impacts of climate change on these olive tree agro-ecosystems.

5 Conclusions

The 10-day period airborne-pollen maps generated using these georeferenced data have allowed the spatio-temporal interpretation of the olive pollen release season across the main Mediterranean cultivation areas. The relationships between maximum pollen emission and latitudinal location have been confirmed, and four spatio-temporal latitudinal categories are presented here. The olive pollen release season starts in the olive-growing areas located at the lowest latitudes, in the last days of April. A defined spatio-temporal pattern in the progression of the pollen release season towards the internal areas is shown here. The highest latitudinal olive cultivation areas can be considered as those that are more relevant to establishing the end of the pollen release season, which takes place towards the end of June.

The major risk days for the people in the occidental Mediterranean who are allergic to olive pollen can be hypothesised as those that are symmetrically distributed around the second 10-day period of May (20 May). Therefore, the maps presented in the present study can be considered to be especially relevant for people allergic to olive pollen.

Acknowledgments The authors are grateful to Ramon Areces Fundation (Spain) for the postdoctoral grant of F. Aguilera.

References

Aguilera, F., & Ruiz-Valenzuela, L. (2009). Study of the floral phenology of *Olea europaea* L. in Jaen province (SE Spain) and its relation with pollen emission. *Aerobiologia, 25*, 217–225.

Aguilera, F., & Ruiz-Valenzuela, L. (2012). Microclimatic-induced fluctuations in the flower and pollen production rate of olive trees (*Olea europaea* L.). *Grana, 51*, 228–239.

Aguilera, F., Ruiz-Valenzuela, L., Fornaciari, M., Romano, B., Galán, C., Oteros, J., et al. (2014). Heat accumulation period in the Mediterranean region: Phenological response of the olive in different climate areas (Spain, Italy and Tunisia). *International Journal of Biometeorology, 58*, 867–876.

Alba, F., Nieto-Lugilde, D., Comtois, P., Díaz-de la Guardia, C., De Linares, C., & Ruiz, L. (2006). Airborne-pollen map for *Olea europea* L. in Eastern Andalusia (Spain) using GIS: Estimation models. *Aerobiologia, 22*, 109–118.

Barranco, D., Fernández-Escobar, R., & Rallo, L. (2008). *El Cultivo del Olivo* (6th ed.). Ediciones Mundi-Prensa: Madrid.

Bonofiglio, T., Orlandi, F., Sgromo, C., Romano, B., & Fornaciari, M. (2009). Evidences of olive pollination date variations in relation to spring temperature trends. *Aerobiologia, 25*, 227–237.

D'Amato, G., Cecchi, L., Bonini, S., Nunes, C., Annesi-Maesano, I., Behrendt, H., et al. (2007). Allergenic pollen and pollen allergy in Europe. *Allergy, 62*, 976–990.

European Aerobiology Society Quality Control Working Group. (2011). Minimum requirements to manage aerobiological monitoring stations included in a national network involved in the EAN. International Association for Aerobiology's Newsletter, 72, 1. https://sites.google.com/site/aerobiologyinternational/iaa-newsletter.

Food and Agriculture Organization. http://faostat3.fao.org. Accessed 11 Dec 2013.

Galán, C., Cariñanos, P., García-Mozo, H., Alcázar, P., & Domínguez-Vilches, E. (2001). Model for forecasting *Olea europaea* L. airborne pollen in South-West Andalusia, Spain. *International Journal of Biometeorology, 45*, 59–63.

Galán, C., García-Mozo, H., Vázquez, L., Ruiz-Valenzuela, L., Díaz-de la Guardia, C., & Domínguez-Vilches, E. (2008). Modelling olive crop yield in Andalucia, Spain. *Agronomy Journal, 100*, 98–104.

García-Mozo, H., Orlandi, F., Galán, C., Fornaciari, M., Romano, B., Ruiz, L., et al. (2008). Olive flowering phenology variation between different cultivars in Spain and Italy: Modelling analysis. *Theoretical and Applied Climatology, 95*, 385–395.

García-Mozo, H., Yaezel, L., Oteros, J., & Galán, C. (2014). Statistical approach to the analysis of olive long-term pollen season trends in southern Spain. *Science of the Total Environment, 473–474*, 103–109.

Giorgi, F., & Lionello, P. (2008). Climate change projections for the Mediterranean region. *Global Planetary Change, 63*, 90–104.

International Olive Council. (2012). Newsletter November. http://www.internationaloliveoil.org.

León-Ruiz, E., García-Mozo, H., Domínguez-Vilches, E., & Galán, C. (2012). The use of the geostatistics in the study of floral phenology of *Vulpia geniculata* (L.) Link. *The Scientific World Journal,*. doi:10.1100/2012/624247.

Menzel, A., & Sparks, T. H. (2006). Temperature and plant development, phenology and seasonality. In J. I. L. Morison & M. D. Morecoroft (Eds.), *Plant growth and climate change* (pp. 70–95). Blackwell Publishing Ltd.

Moriondo, M., Trombi, G., Ferrise, R., Brandani, G., Dibari, C., Ammann, C. M., et al. (2013). Olive trees as bio-indicators of climate evolution in the Mediterranean Basin. *Global Ecology and Biogeography, 22*, 818–833.

Orlandi, F., García-Mozo, H., Ben Dhiab, A., Galán, C., Mssallem, M., & Fornaciari, M. (2014). Olive tree phenology and climate variations in the Mediterranean area over the last two decades. *Theoretical and Applied Climatology, 115*, 207–218.

Orlandi, F., García-Mozo, H., Galán, C., Romano, B., Díaz-de la Guardia, C., Ruiz, L., et al. (2010). Olive flowering trends in a large Mediterranean area (Italy and Spain). *International Journal of Biometeorology, 54*, 151–163.

Orlandi, F., Vázquez, L., Ruga, L., Bonofiglio, T., Fornaciari, M., García-Mozo, H., et al. (2005). Bioclimatic requirements for olive flowering in two Mediterranean regions located at the same latitude (Andalucia, Spain, and Sicily, Italy). *Annals of Agricultural and Environmental Medicine, 12*, 47–52.

Oteros, J., Orlandi, F., García-Mozo, H., Aguilera, F., Ben Dhiab, A., Bonofiglio, T., et al. (2013). Better prediction of Mediterranean olive production using pollen-based models. *Agronomy for Sustainable Development, 34*(3), 685–694.

Salmi, T., Määttä, A., Anttila, P., Ruoho-Airola, T., & Amnell, T. (2002). Detecting trends of annual values of atmospheric pollutants by the Mann-Kendall test and Sen's slope estimates—the Excel template application Makesens. Publications on Air Quality No. 31. Finnish Meteorological Institute. Helsinki, Finland.

Sibson, R. (1981). A brief description of natural neighbor interpolation. In Interpreting Multivariate (Ed.), *Barnett V* (pp. 21–36). Data: John Wiley and Sons.

Sirois, A. (1998). A brief and biased overview of time series or how to find that evasive trend. In WMO report No. 133: WMO/EMEP workshop on Advanced Statistical methods and their application to Air Quality Data sets (Helsinki, 14–18 Sept 1998).